Available online at www.sciencedirect.com
SCIENCE DIRECT
Journal of Catalysis 229 (2005) 55–63
JOURNAL OF CATALYSIS
www.elsevier.com/locate/jcat

Combined in situ attenuated total reflection infrared and UV–vis spectroscopic study of alcohol oxidation over Pd/Al_2O_3

Thomas Bürgi *

Institut de Chimie, Université de Neuchâtel, Rue Emile-Argand 11, 2007 Neuchâtel, Switzerland

Received 16 August 2004; revised 6 October 2004; accepted 8 October 2004

Abstract

In situ attenuated total reflection (ATR) infrared and UV–vis spectroscopy are combined to yield simultaneous time-resolved information on dissolved reaction products, adsorbed species, and the catalyst during the oxidation of ethanol and 2-propanol on a 5% Pd/Al_2O_3 catalyst. The oxidation is initiated by change from hydrogen- to oxygen-saturated solvent flow. 2-Propanol oxidation is observed only in the transient period, whereas ethanol oxidation is also observed in the steady state. This may be ascribed to overoxidation of the catalyst in the former case. In a mixture of the two alcohols the same thing is observed. Competitive adsorption in the steady state may explain this behavior. For ethanol oxidation ethyl acetate is also observed during the transient period. The UV–vis spectra reveal a fast reversible change of the catalyst with switching between hydrogen and oxygen and a slow irreversible change during ethanol oxidation. The latter is ascribed to the change in Pd particle structure, which hardly affects, however, catalyst activity on the time scale of about 1 h.

Keywords: In situ spectroscopy; Alcohol oxidation; Attenuated total reflection; UV–vis; Reaction mechanism; Catalyst deactivation; Ethyl acetate; Ethanol; 2-Propanol; Overoxidation

1. Introduction

In situ spectroscopy and *operando* spectroscopy of catalytic interfaces provide in-depth molecular level information on reaction mechanisms and catalyst behavior [1] and thus pave the way for the rational design of catalyst materials and processes. This has recently stimulated the development and application of in situ spectroscopic techniques in heterogeneous catalysis. Considerable effort has been devoted to solid–gas interfaces, whereas catalytic solid–liquid interfaces have been studied to a lesser extent by in situ spectroscopic techniques, despite their importance for a variety of relevant processes.

Attenuated total reflection (ATR) infrared spectroscopy [2] has been successfully applied to the study of processes at solid–liquid interfaces of model [3–6] and real powder catalysts [7,8]. The ATR technique makes use of the evanescent electromagnetic field in the vicinity of an optical element and eliminates excessive solvent absorption. Simultaneous information on dissolved molecules, such as reactants and products, and on species adsorbed to the catalyst surface, such as intermediates [9] and catalyst poisons [10], can be obtained. The ATR technique can also provide information on the catalyst itself, depending on the nature of the latter [8,11]. Among the strengths of ATR spectroscopy for the investigation of catalytic processes is the excellent time resolution of Fourier transform infrared spectroscopy [12], making it possible to follow relatively fast processes when appropriately designed cells are used [13]. The challenges are connected with the sensitivity and complexity of catalytic solid–liquid interfaces [7,8].

In this contribution we combine the ATR technique with in situ UV–vis spectroscopy. The simultaneous application of two complementary techniques is expected to yield further insight into the processes occurring at the catalytic interface [14]. In particular, ATR infrared spectroscopy gives

* Tel.: +41-32-718-24-12; fax: +41-32-718-25-11.
E-mail address: thomas.burgi@unine.ch.

0021-9517/$ – see front matter
doi:10.1016/j.jcat.2004.10.016

primarily information on the chemical nature of dissolved and adsorbed species, whereas UV–vis spectroscopy can be used to probe catalytic sites [15].

The combined IR/UV–vis technique is applied to the study of alcohol oxidation over a Pd/Al_2O_3 catalyst. Selective oxidation of alcohols over noble metal catalysts proceeds under mild conditions and is an attractive synthetic route for fine chemical production [16–20]. Catalyst deactivation, which can have different origins, as discussed in detail in recent reviews on alcohol oxidation [16,19], remains a challenge. Processes like corrosion, restructuring, and leaching of the active metal during reaction could affect catalyst performance. A thorough understanding of these phenomena and their interplay calls for adequate in situ analytical methods. UV–vis spectroscopy is a sensitive probe for metal particles and is therefore a promising tool for shedding light on processes that directly affect the catalyst.

The present manuscript is organized as follows. In Section 2 the new setup for simultaneous ATR-IR and UV–vis spectroscopy is described. In Section 3 time-resolved ATR-IR spectra are first presented for the oxidation of ethanol, a primary alcohol, and mixtures of ethanol and 2-propanol, the latter being a secondary alcohol. These experiments reveal the species that are present at the catalytic solid–liquid interface and show which reactions occur. Furthermore, the time dependence of the ATR signals gives insight into the kinetics of the different processes occurring on the catalyst. UV–vis spectra that indicate changes in the Pd catalyst particles during oxidation are then presented. The discussion focuses on the reasons for the different behaviors of ethanol and 2-propanol with respect to reaction network and kinetics and the possible origin of the observed changes of the Pd particles during oxidation, as indicated by the UV–vis measurements.

2. Experimental

2.1. Catalyst and chemicals

A 5% Pd/Al_2O_3 catalyst (Johnson Matthey, Type 324, mean particle size 3.4 nm as determined by TEM) was used. Before measurements the catalyst was reduced in situ by flowing hydrogen-saturated ethanol. Ethanol (Merck p.a.) and 2-propanol (Merck p.a.) were used as supplied. Nitrogen (99.995%), hydrogen (99.995%), and oxygen (99.998%) gases were used to saturate the liquids. All gases were supplied by CarbaGas.

2.2. Thin-film preparation

A slurry of the catalyst powder was prepared from about 20 mg catalyst and 5 ml ethanol (2-propanol in the case of 2-propanol oxidation). We prepared films of the catalyst powder by dropping the slurry onto a ZnSe internal reflection element (IRE) (52 × 20 × 2 mm; KOMLAS). The solvent was allowed to evaporate, and the procedure repeated totally three times. After drying for several minutes at 40 °C in air, loose catalyst particles were removed by flowing ethanol (2-propanol) over the IRE. After drying in air the film was ready for use. The amount of catalyst exposed to the solvent was between 1 and 1.5 mg.

2.3. In situ spectroscopy

ATR spectra were recorded with a dedicated Teflon flow-through cell with a volume of 0.077 ml and a gap between IRE and the surface of the cell of 250 μm [7]. The cell has two inlets, which allows the fast exchange between two different fluids. The cell was mounted on an attachment for ATR measurements (Wilks Scientific) within the sample compartment of a Bruker Equinox-55 FTIR spectrometer equipped with a MCT detector. Spectra were recorded at 4 cm^{-1} resolution.

The ATR cell is equipped with a fused silica window (5-mm diameter and 3-mm thickness), which allows simultaneous recording of UV–vis and ATR-IR spectra of the catalyst layer. The distance between inlet and outlet of the ATR cell is 36 mm, and the window for UV–vis spectroscopy is positioned 10 mm from the outlet. A UV–vis probe was positioned in front of the window perpendicular to the IRE surface, such that the end of the probe was located approximately 4 mm above the catalyst layer. The probe (Avantes) consisted of six fibers that guided the light from a deuterium halogen source to the sample and one fiber that guided the reflected light to a UV–vis spectrometer (Avantes, 2.4-nm resolution) equipped with a 2024-pixel CCD detector array. The typical integration time for one spectrum was 100 ms.

Alternatively, the UV–vis spectrometer can be used to record spectra for the ATR cell effluent [9]. The latter is directly coupled into a home-built UV–vis flow-through cell consisting of two stainless-steel tees connected with a Teflon tube. The light from the source is guided to one end of the cell via fiber optics. The transmitted light is collected at the other side of the cell and coupled into a second fiber, which guides the light to the UV–vis spectrometer. The typical integration time for one transmission spectrum was 10 ms. The path length of the UV–vis transmission cell was 4 cm.

The solvent was saturated with gases in two separate glass bubble tanks and was passed through the cells and over the sample by means of a peristaltic pump (Ismatec, Reglo 100) located after the UV–vis transmission cell. Flow rates between 0.3 and 2.5 ml/min were used. Two pneumatically actuated three-way Teflon valves (Parker PV-1-2324) were used to control the solvent flow from the two tanks. All experiments were performed at 30 °C. Stainless-steel and Teflon tubing was used. A schematic of the experimental setup is given in Fig. 1.

2.4. Measurement protocol and data acquisition

The catalyst system was stimulated by the periodic admission of ethanol (2-propanol) saturated with hydrogen and oxygen. During one modulation period (flow of hydrogen-saturated ethanol followed by an equally long flow of

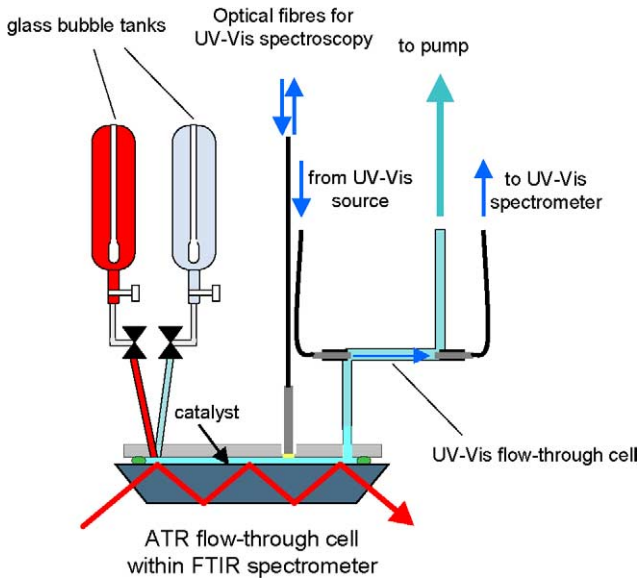

Fig. 1. Schematic setup of the combined in situ attenuated total reflection (ATR) and UV–vis experiment with fiber optics for on-line UV–vis analysis.

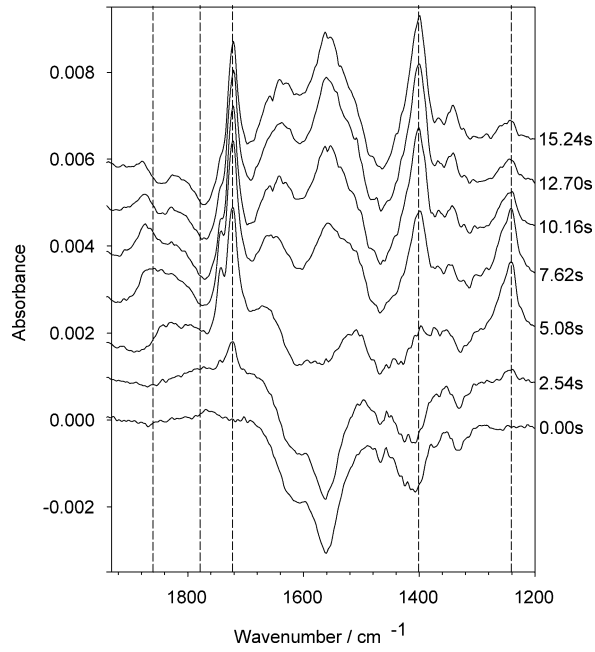

Fig. 2. Time-resolved ATR spectra of the catalytic solid–liquid interface of a 5% Pd/Al_2O_3 catalyst in contact with ethanol. The spectra were recorded during a modulation experiment, where ethanol saturated with H_2 and O_2 was flowed alternately over the sample. The reference was recorded while flowing H_2-saturated solvent. At the right margin the time after switching to O_2 flow is indicated. The vertical lines indicate some signals that are shown as a function of time in Fig. 3. The modulation period was $t = 153$ s. Flow rate 1.1 ml/min. The signal was averaged over five modulation periods.

oxygen-saturated ethanol) 60 infrared spectra were recorded at a sampling rate of 40 kHz, with the use of the rapid scan function of the FTIR spectrometer. For each spectrum several scans were averaged. Three modulation periods were applied before data acquisition was started. Infrared spectra were then averaged over five periods. UV–vis (of catalyst or effluent) and ATR-IR spectra were recorded simultaneously and synchronized. Before every scan of the IR spectrometer the UV–vis spectrometer was triggered to record one scan. Several scans were averaged such that for one modulation period a total of 60 spectra were obtained.

Experiments were typically performed as follows. Ethanol in the two glass bubble tanks was saturated with nitrogen before one tank was saturated with hydrogen and one with oxygen. Hydrogen-saturated ethanol was then passed first over the sample for 10 min. Afterward the flow was changed between hydrogen- and oxygen-saturated ethanol five times (each flow for about 1 min). After that treatment, modulation experiments were started. Several consecutive modulation experiments were performed with the same catalyst layer. The catalyst layer was freshly prepared every day, however.

3. Results

Fig. 2 shows time-resolved ATR spectra recorded after the flow at the entrance of the cell was switched from H_2- to O_2-saturated solvent. The reference was recorded in hydrogen 50 s before switching. Several signals of dissolved and adsorbed species evolved within the first couple of seconds. Bands associated with CO adsorbed to the Pd catalyst can be observed between 1800 and 1900 cm^{-1}. The band at 1724 cm^{-1} is associated with dissolved acetaldehyde, the primary oxidation product of ethanol. At the higher frequency side of this band a signal appears at

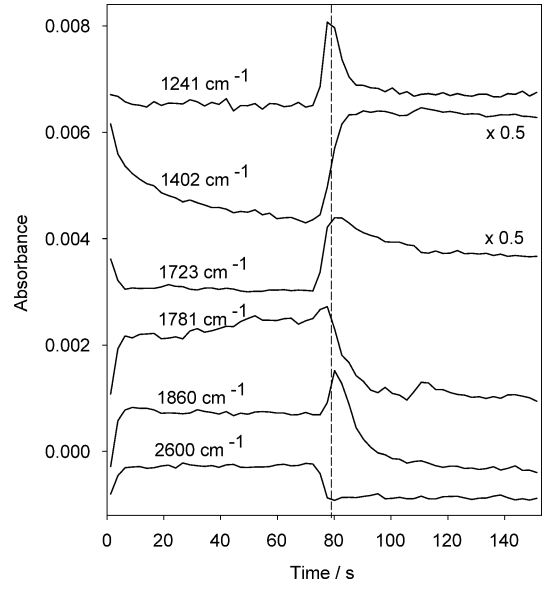

Fig. 3. Time-dependence of some ATR signals during one modulation period for the experiment shown in Fig. 2.

about 1742 cm^{-1}, which is strongly attenuated after 10 s. At 1240 cm^{-1} a band with similar time behavior is observed. Finally, the broad bands centered at 1560 and 1400 cm^{-1} are mainly associated with acetate on the catalyst support [8,21]. Fig. 3 shows the time dependence of some ATR signals for the same experiment. At time $t = 0$ the flow was switched

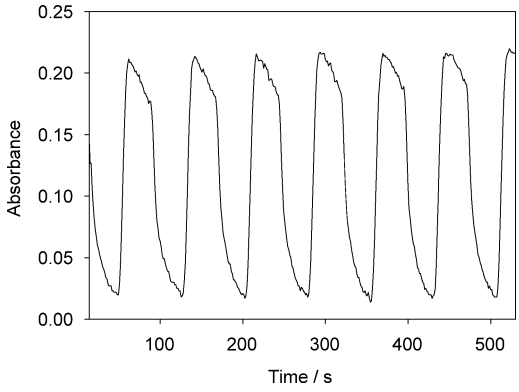

Fig. 4. Time-dependence of the UV signal at 300 nm associated with acetaldehyde in the ATR cell effluent. The measurement was performed on-line during an ATR experiment with modulation period $T = 76$ s, flow rate 1.1 ml/min.

from O_2- to H_2-saturated ethanol. The spectra shown in Fig. 2 correspond to the time interval between $t = 76.5$ and 91.7 s. The signal at 2600 cm^{-1}, far from any significant molecular absorption band, reflects the response of the catalyst to the hydrogen and oxygen. Dissociative adsorption of the two molecules on the Pd catalyst leads to a slight change in the optical constants of the metal. As a consequence the absorption signal over the whole infrared region reversibly increases in hydrogen and decreases in oxygen, as discussed in detail elsewhere [8]. The species absorbing at 1240 and 1742 cm^{-1} has a time behavior that is significantly different from that of the primary oxidation product acetaldehyde, which absorbs at 1724 cm^{-1}. The former signals are significant only for a change from hydrogen- to oxygen-saturated ethanol flow, whereas the acetaldehyde signal increases for a switch to oxygen and then decreases fast to a steady-state value. The signal at 1860 cm^{-1} associated with carbon monoxide on Pd initially increases for a switch to oxygen, because of decarbonylation of the aldehyde, and then decreases because of oxidation of CO by oxygen. The signals at 1402 and 1560 due to acetates [22] on the support demonstrate that the acetaldehyde can be further oxidized to acetic acid.

Fig. 4 shows the UV signal at 300 nm (acetaldehyde) of the ATR-cell effluent as a function of time during several modulation periods. The signal demonstrates that the process is reversible over several consecutive modulation periods. The figure furthermore confirms that during the switch to oxygen the formation rate of acetaldehyde is initially high and then decreases slightly. During the switch to hydrogen the signal vanishes.

Fig. 5 shows ATR spectra for the same type of experiment as shown in Fig. 2, however, now with a mixture of ethanol and 2-propanol (50 vol% each). In the carbonyl stretching region between 1700 and 1750 cm^{-1} three signals are observed (Fig. 5, right). The signal at 1712 cm^{-1}, which was not observed in the experiment in neat ethanol, belongs to acetone, the oxidation product of 2-propanol. Acetone has another characteristic absorption band at 1358 cm^{-1}. Com-

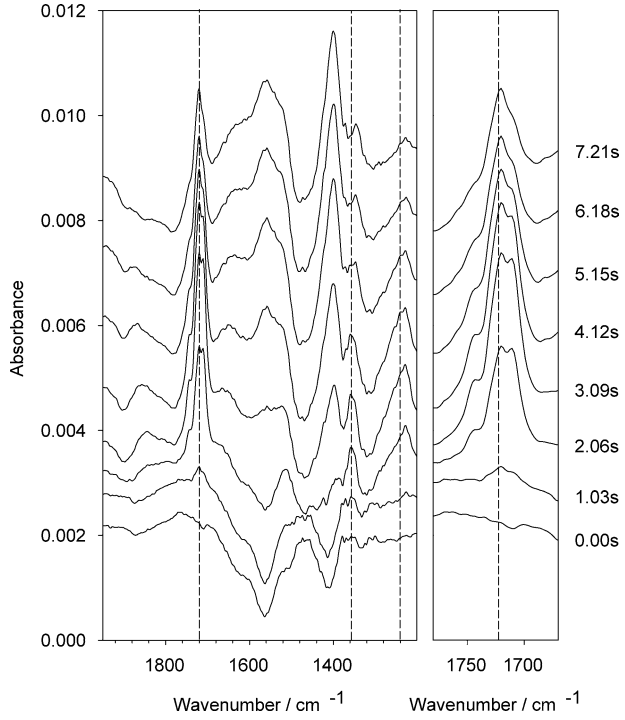

Fig. 5. Time-resolved ATR spectra of the catalytic solid–liquid interface of a 5% Pd/Al_2O_3 catalyst in contact with an ethanol/2-propanol mixture (50 vol% each). The spectra were recorded during a modulation experiment, where the mixture saturated with H_2 and O_2 was flowed alternately over the sample. The reference was recorded in hydrogen. The time given at the right margin indicates the time after switching to O_2 flow. An expansion of the carbonyl stretching region is depicted in the right part of the figure. The vertical lines indicate some signals that are shown as a function of time in Fig. 6. The modulation period was $T = 61$ s. Flow rate 1.5 ml/min. The signal was averaged over eight modulation periods.

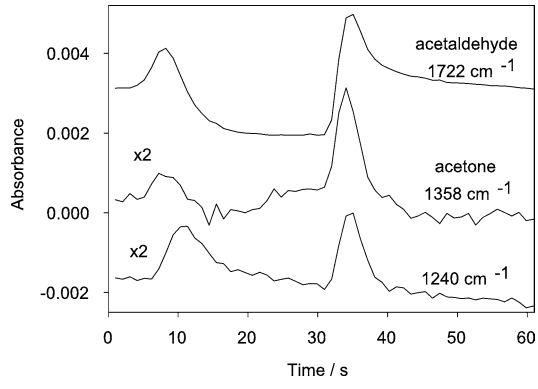

Fig. 6. Time-dependence of some ATR signals during one modulation period for the experiment shown in Fig. 5.

parison of Figs. 2 and 5 shows that the signals due to CO and acetate that were observed in the case of neat ethanol (Fig. 2) are also observed in the ethanol/2-propanol mixture. Fig. 6 shows the signals associated with acetaldehyde, acetone, and the species giving rise to the bands at 1742 and 1240 cm^{-1} as a function of time. Acetone is observed in significant amounts only for the switch between oxygen and hydrogen and vice versa. This behavior was already ob-

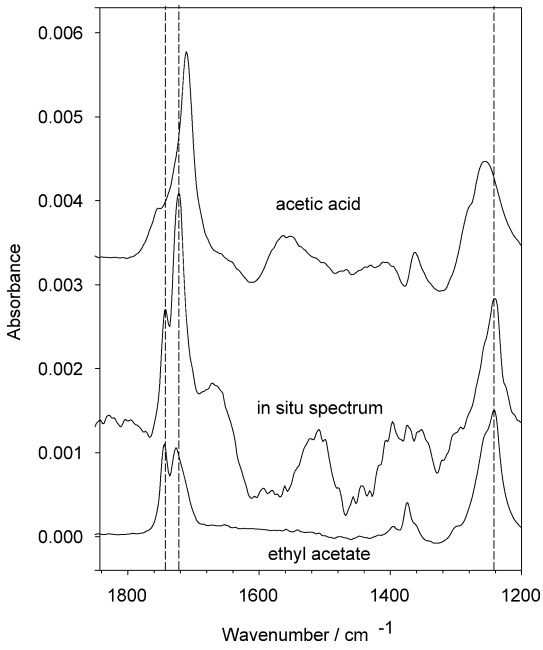

Fig. 7. ATR spectra of acetic acid and ethyl acetate dissolved in ethanol. The spectra were recorded over a clean ZnSe internal reflection element. The reference was recorded in neat ethanol. For comparison an in situ ATR spectrum of a Pd/Al_2O_3 catalyst in contact with ethanol is shown. The spectrum was recorded five seconds after switching to O_2-saturated ethanol (see Fig. 2 for more details).

served for experiments with neat 2-propanol [8]. The signal at 1724 cm^{-1}, which is mainly associated with acetaldehyde, also has maxima during the switching, part of which may be due to signal overlap. Significant acetaldehyde formation is observed in an oxygen atmosphere, in contrast to acetone formation.

The carbonyl stretching region shown in Fig. 5 (right), with the signals from acetaldehyde, acetone, and the species associated with the band at 1742 cm^{-1}, exhibits significant changes during the transient period during the switch from hydrogen- to oxygen-saturated solvent. Initially all signals increase, but after a short time the signal at 1742 cm^{-1} and the one at 1712 cm^{-1} associated with acetone decrease much faster than the acetaldehyde signal. The former signals virtually vanish after some time, whereas the one due to acetaldehyde remains significant in the presence of oxygen.

With the exception of the bands at 1742 and 1242 cm^{-1}, the signals in the ATR spectra discussed above can be explained by the oxidation of the alcohol to aldehyde and ketone, respectively, and the oxidation and decarbonylation reactions of the aldehyde. In the following the identification of the species associated with the 1742 and 1242 cm^{-1} bands is sought. A possible candidate from a chemical point of view is dissolved acetic acid. If water is present in the reaction medium, the aldehyde can be hydrated to the geminal diol, which is subsequently fast dehydrogenated to the acid on the catalyst surface [16,23]. Water is certainly present in small amounts. The dissociative adsorption of the alcohol leads to adsorbed hydrogen and an alkoxide. For 2-propanol oxidation on Pd/Al_2O_3 the corresponding alkoxide was recently indicated by in situ ATR spectroscopy [9]. The oxidation of hydrogen by the dissociatively adsorbed oxygen leads to water [8]. Acid formation is clearly indicated by the bands at around 1400 and 1560 cm^{-1} associated with acetate species adsorbed on the Al_2O_3 support [22,24]. However, acetic acid dissolved in ethanol is not compatible with the spectra measured in situ, as revealed by Fig. 7, where the ATR spectrum of dissolved acetic acid and the in situ spectrum are compared. Fig. 7 shows that the two strongest bands of dissolved ethyl acetate match the two signals at 1742 and 1240 cm^{-1} (Fig. 2) in an excellent way. The second carbonyl band of ethyl acetate at lower wavenumbers is superimposed on the acetaldehyde band. Table 1 summarizes the infrared signals observed in the ATR experiments.

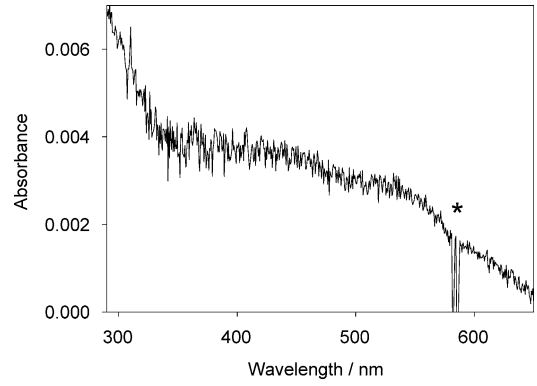

Fig. 8. UV–vis spectrum of the 5% Pd/Al_2O_3 catalyst, recorded while flowing ethanol. The spectrum highlights the changes induced by the switching of the dissolved gas from hydrogen to oxygen. The spectrum was recorded in oxygen, whereas the reference was recorded 60 s before in hydrogen. The spectrum represents an average over five modulation periods. Flow rate 0.85 ml/min. The asterisk indicates a region in the spectrum, where the detector was saturated.

Fig. 8 shows a UV–vis spectrum recorded during a modulation experiment (hydrogen–oxygen) in ethanol. The spectrum was recorded while oxygen-saturated ethanol flowed over the sample, whereas the reference spectrum was recorded in hydrogen-saturated ethanol. The change in the gas had a small but significant effect on the spectra. This change was reversible, as demonstrated by Fig. 9, where the absorbance at 400 nm is plotted as a function of time during a modulation experiment. The absorbance at 400 nm increased for a flow of O_2-saturated ethanol and decreased again in H_2-saturated ethanol.

The change of the UV–vis spectrum stimulated by change of the dissolved gas, as shown in Figs. 8 and 9, is fast, on the order of seconds. However, we have also noticed slower changes in the UV–vis spectra of the catalyst. Fig. 10 shows UV–vis spectra recorded during the flow of, first, hydrogen-saturated ethanol for 30 min (three bottom spectra), followed by oxygen-saturated ethanol (three top spectra). In hydrogen the spectrum hardly changes. Possibly part of the slight change is due to drifts of the instrument during the relatively long experiment. However, in oxygen the spectrum changes significantly. The inset of Fig. 10 shows the absorbance at

Table 1
Observed signals and assignment for the in situ ATR experiments during ethanol and 2-propanol oxidation

Wavenumber (cm^{-1})	Species	Assignment
1241	Ethyl acetate, dissolved	ν(C–O)
1358	Acetone, dissolved	$\delta(CH_3)$
1402	Acetate, adsorbed on Al_2O_3	$\nu_s(COO^-)$
1560	Acetate, adsorbed on Al_2O_3	$\nu_{as}(COO^-)$
1640	Water, adsorbed on Al_2O_3	δ(HOH)
1712	Acetone, dissolved	ν(C=O)
1724	Acetaldehyde, dissolved	ν(C=O)
1742	Ethyl acetate, dissolved	ν(C=O)
1781	Carbonyl species adsorbed on Pd	ν(CO)
1860	CO adsorbed on Pd	ν(CO)
2600	Metal	(Broad absorption over the whole mid IR)

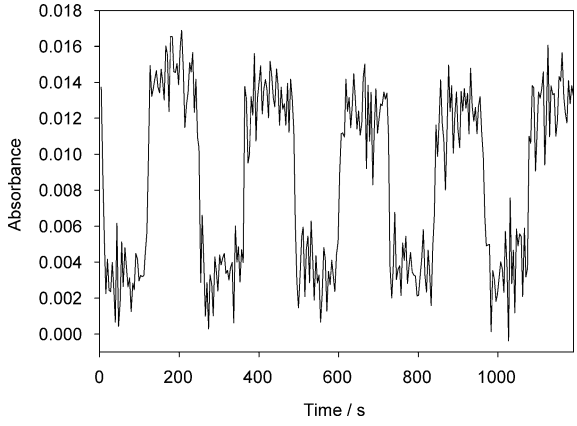

Fig. 9. Absorbance at 400 nm as a function of time for a modulation experiment, where hydrogen- and oxygen-saturated ethanol was alternately flowed over the Pd/Al_2O_3 catalyst. Flow rate 0.85 ml/min. The absorbance increased in oxygen and decreased in hydrogen.

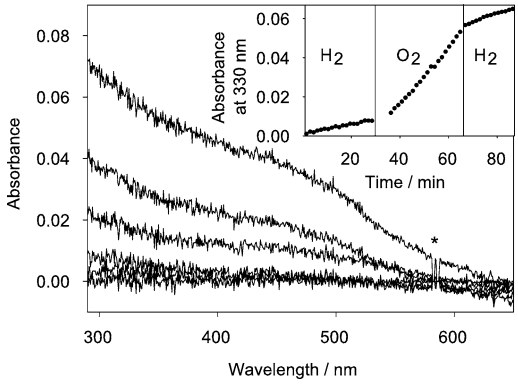

Fig. 10. UV–vis spectra of the 5% Pd/Al_2O_3 catalyst. The reference was recorded at $t = 0$ while flowing hydrogen-saturated ethanol. The three bottom spectra were recorded while flowing hydrogen-saturated ethanol at $t = 1$, 15 and 30 min. The three top spectra were recorded while flowing oxygen-saturated ethanol at $t = 40$, 49 and 66 min. The inset shows the absorbance at 330 nm as a function of time. The spectra represent averages of 200 scans with 100 ms accumulation time each. Flow rate 0.3 ml/min.

400 nm as a function of time. As becomes evident, the slow changes in the UV–vis spectra are not reversible in hydrogen. During the experiment acetaldehyde was observed by ATR, as evidenced by the band at 1724 cm^{-1} in the presence of oxygen. During 35 min of oxygen flow the acetaldehyde signal decreased only slightly (on the order of 10% or less) after the transient period. Identical experiments without catalyst did not result in the UV–vis features described above.

4. Discussion

In the following discussion the formation of ethyl acetate is first briefly addressed. Then the different behavior of ethanol and 2-propanol and their competitive oxidation is discussed in view of overoxidation of the catalyst and catalyst potential. Finally the observed changes in the UV–vis spectra are discussed, and it will be argued that the signals arise because of redispersion of the Pd particles during the oxidation reaction.

The ATR spectra in Figs. 2 and 5 exhibit the formation of ethyl acetate during ethanol oxidation. The mechanism of ester formation can be manifold. One possible pathway for ethyl acetate formation involves formation of the acid and its subsequent esterification. Since this does not happen in solution to a significant extent (Fig. 7; see spectrum of acetic acid in ethanol), involvement of the catalyst is likely. Another pathway is the direct conversion of the aldehyde to the carboxylic ester. The latter reaction is observed when aldehydes are treated with ozone in the presence of an alcohol [25]. The activated oxygen on the Pd catalyst could assume the role of ozone in a similar reaction.

The several observed adsorbed and dissolved species show distinctly different responses toward the stimulation, that is, the change in dissolved gas. Ethyl acetate is formed in significant amounts only transiently during the switch from hydrogen- to oxygen-saturated ethanol and possibly, to a much lesser extent, during the switch back, as shown in Fig. 3 (absorbance at 1241 cm^{-1}). A similar behavior was previously observed for the formation of acetone from 2-propanol in the same type of experiment under identical conditions [8,9]. On the other hand, acetaldehyde is produced also after the transient period in the presence of dissolved oxygen. As mentioned above, dissolved acetic acid

is not directly observed, but the acetate adsorbed on the Al_2O_3 is. The acetate signals (1402 cm^{-1} in Fig. 3) increase fast only in the transient period within a few seconds. When alumina is exposed to dissolved acetic acid the ATR signals keep growing for a considerably longer time [24]. The time behavior of the acetate signals in our experiments therefore indicates that acetic acid is formed in significant amounts only during the short transient period with switching between hydrogen- and oxygen-saturated solvent. During that time water formation is expected to be most significant, because of the addition of supplementary hydrogen to the system, and acid can form via hydration of acetaldehyde. Fig. 3 shows that ethyl acetate is formed in significant amounts only when the signals from acetates on the support strongly increase, that is, when acetic acid is present. This supports a mechanism of ethyl acetate formation via acetic acid.

The different behavior of 2-propanol and ethanol will be discussed next. Whereas acetone formation is observed only in the transient period, with the change between hydrogen- and oxygen-saturated solvent [8,9], acetaldehyde formation is also observed in the steady state in the presence of oxygen (Fig. 3). This could be due to the different reactivities of the two alcohols (primary and secondary alcohol). If the reaction of 2-propanol proceeds too slowly after the initial period, the catalyst runs into the overoxidized state, where further adsorption of the reactant is limited by dissociatively adsorbed oxygen. For the faster reacting ethanol this may not happen. It has been shown recently that one role of oxygen is the oxidation and removal of by-products from the catalyst surface [10]. One possible difference between the two alcohols may be the different extent of poisoning of the Pd surface. It has been shown that 2-propanol can decompose to form CO and furthermore can react on oxygen-covered Pd to form acetate in ultrahigh vacuum conditions [26]. Under the conditions of our experiments these reactions are not observed for 2-propanol [8,9]. However, for ethanol both CO and acetate are formed (see Fig. 2). This therefore strongly indicates that stronger poisoning of the catalyst in the case of 2-propanol compared with ethanol is not the reason for their vastly different overall reactivity. The experiment in which a 50:50 vol% mixture of 2-propanol and ethanol was used (Figs. 5 and 6) gives more insight into these issues.

Despite the fact that the catalyst is not in an overoxidized state, as the ethanol oxidation activity shows, no significant 2-propanol oxidation is observed after the transient period. Several factors could account for this observation. Competitive dissociative adsorption of the two alcohols could hinder adsorption of 2-propanol. The initial adsorption steps lead to the corresponding alkoxides, ethoxide and 2-propoxide, respectively [9]. The relative adsorption strengths of the two alkoxides determine their relative abundance on the catalyst surface, provided that adsorption/desorption equilibrium is established or nearly established between the dissolved alcohols and the adsorbed alkoxides. Substrates with high adsorption strength may also compete with oxygen adsorption. For the oxidation of 5-hydroxymethylfurfural on platinum-group metals, for example, no overoxidation was found, which was attributed to the strong adsorption of the substrate, caused by the interaction of the π-electrons of the furan moiety [27]. Under the applied experimental conditions 2-propanol cannot compete with oxygen adsorption. In situ ATR experiments revealed that the 2-propoxide intermediate is observed in significant amounts only during the short transient period, with the switch between hydrogen and oxygen [9]. Therefore competitive adsorption between the alcohols may be why no significant 2-propanol oxidation is observed after the transient period, whereas ethanol oxidation is. In the transient period both alcohols are oxidized at a significant rate, which indicates a rather different state of the catalyst surface during that time.

Each Pd particle can be viewed as a “short-circuited” electrochemical cell [28] in which the anodic (alcohol oxidation) and cathodic (oxygen reduction) half-reactions take place at the same rate and potential (“mixed potential”) [29]. Induced by the change of the dissolved gas from hydrogen to oxygen, the potential is swept to higher values. The observations can therefore be interpreted in terms of this potential sweep. At relative low potential of the catalyst in the transient period, both alcohols are oxidized at a significant rate, whereas at higher catalyst potential (steady state) only ethanol is oxidized at an appreciable rate. The relative oxidation rates of the two alcohols can therefore be tuned by adjustment of the catalyst potential (oxygen supply). Similarly, the selectivity in ethanol oxidation (oxidation products acetaldehyde, acetic acid, and ethyl acetate) is strongly potential dependent. Indeed, for the oxidation of cinnamyl alcohol and cinnamaldehyde with oxygen over a 0.9 wt% Bi–5 wt% Pt catalyst, different catalyst potentials were measured [28].

The changes in the Pd particles as indicated by the UV–vis spectra are discussed in the final paragraphs. Clearly the state of the catalyst is different in hydrogen and oxygen and during the transient period, during switching between hydrogen and oxygen. This change, which is reflected in catalytic activity, is also observed in the UV–vis spectrum, as revealed by Fig. 8. The change in the UV–vis spectrum, with the change in the dissolved gas, is fast and reversible (Fig. 9). A similar effect is observed in the ATR spectra (see Fig. 3, absorbance at 2600 cm^{-1}). Based on reflectivity calculations, these changes were assigned to slight oxidation and reduction, respectively, of Pd in the presence of oxygen and hydrogen, respectively [8]. We ascribe the observed changes in the UV–vis spectrum (Figs. 8 and 9) to a similar effect.

Fig. 10 reveals significant alteration of the UV–vis spectrum in oxygen while the catalyst is active. As stated above, the activity decreased only slightly during the oxygen flow of 30 min. The slow changes in the UV–vis spectrum of the catalyst in oxygen could have different origins. One possibility is corrosion of Pd, which was reported for a $Pd/CaCO_3$ catalyst [30]. The metal content decreased from 4.3 to 1.1% after the catalyst was reused 16 times in the partial oxidation of 2-methylphenoxyethanol to 2-methylphenoxyacetic acid,

whereas the reaction rate was not affected by the corrosion. A significant loss of the strongly absorbing metal should lead to a decrease in the absorbance in the UV–vis spectra. We therefore conclude that the observed change in the spectra (Fig. 10) is not primarily due to the loss of Pd.

Alternatively, deactivation of platinum catalysts (Pt/C) during alcohol oxidation was attributed to the penetration of oxygen atoms into the platinum lattice [31,32]. This process was relatively slow. During the first 14 h the rate for D-gluconate oxidation decreased to about one-half of the initial rate. Penetration of oxygen into the bulk metal was also reported for Pd [33]. Based on kinetic experiments and the study of different start-up procedures, Dijkgraaf and coworkers concluded that the observed deactivation was due to oxygen but not to the formation of a Pt oxide [32]. The authors proposed formation of a phase of dissolved oxygen.

The formation of palladium oxide as the cause for the observed spectral changes (Fig. 10) is also unlikely in our experiments, based on the comparison with UV–vis spectra of palladium oxide [34]. More importantly, the observed changes resist subsequent flow of dissolved hydrogen, as the inset in Fig. 10 shows. Under the applied conditions oxidized palladium is readily reduced to metallic palladium [8]. Therefore, the principal changes in the UV–vis spectrum in the presence of oxygen are not due to the formation of palladium oxide. The dissolution of oxygen into the Pd lattice during exposure to oxygen cannot be excluded, but the observation that the spectral changes are not readily reversible in hydrogen is an argument against such a conclusion.

Redispersion and changes in particle size could also result in spectral changes. Small Pd particles exhibit strongly increasing absorbance at decreasing wavelength [35], in agreement with the first term of Mie theory [36]. It has been found for Pt and Pd particles that the quantity $S = -d\log\varepsilon/d\log\lambda$, where ε is the molar extinction coefficient and λ is the wavelength of the light, depends on particle size [37]. The general appearance of the spectra in Fig. 9, with the strong increase in absorbance at lower wavelength, could thus be an indication of change in particle size. A possible scenario is the dissolution of Pd and subsequent redeposition (Ostwald ripening) [38]. Pd dissolution is mediated by strongly chelating species such as carboxylic acids and high catalyst potential (high oxygen coverage) [39,40]. Such a mechanism would explain the irreversible nature of the process monitored by in situ UV–vis spectroscopy.

The observation that the activity is hardly affected within the time of our experiments, whereas significant changes are observed in the UV–vis spectra, is intriguing at first glance. However, alcohol oxidation in the transport-limited regime results in considerable gradients within the catalyst particle. Depending on local concentration of dissolved oxygen, the Pd particles may be more or less covered by oxygen. Particles covered heavily by oxygen do not contribute much to the catalytic activity but are prone to Pd dissolution, which may be the explanation for the observation that the catalyst is changing (as observed by UV–vis) without much affecting activity (as observed by ATR-IR).

5. Conclusion

We have combined in situ attenuated total reflection infrared (ATR-IR) and UV–vis spectroscopy to study alcohol oxidation on a Pd/Al_2O_3 catalyst. The two methods provide complementary information. ATR is used to identify dissolved reaction products and species adsorbed to catalyst and support, whereas UV–vis is sensitive to changes of the catalyst.

During the oxidation of ethanol, several species are observed at the interface. Oxidation is evidenced by the presence of dissolved acetaldehyde, which is the primary oxidation product. Further oxidation to acetic acid is confirmed indirectly by the appearance of signals associated with acetates on the Al_2O_3 support, whereas the concentration of dissolved acetic acid is too low to be clearly detectable. Decarbonylation of acetaldehyde leads to carbon monoxide on the Pd. Furthermore, the ATR spectra indicate the presence of dissolved ethyl acetate.

When the catalyst system was stimulated by periodic variation of the dissolved gas between hydrogen and oxygen two, distinctly different regimes were observed: a transient region during the switching and a steady state. Ethyl acetate is observed only in the transient region. Moreover, the signal from the acetates on the support increases quickly only during the transient region. Acetaldehyde is observed in significant amounts also in the steady state, but the signal is highest in the transient region.

Under identical conditions 2-propanol oxidation does not proceed to a significant extent beyond the transient region, which may be ascribed to overoxidation of the catalyst. In a mixture of 2-propanol and ethanol the former is not oxidized to a significant extent in the steady state either, despite the fact that the catalyst is not in an overoxidized state, as significant oxidation of the latter demonstrates. Competitive adsorption of the two alcohols may account for this observation. However, during the transient region the two alcohols are oxidized simultaneously.

In situ UV–vis spectroscopy reveals changes on different time scales. Fast reversible changes are observed during the switch from hydrogen to oxygen and are ascribed to changes in the optical properties of the Pd particles due to adsorption of hydrogen and oxygen. A considerably slower irreversible change in the spectra is observed during oxidation during oxygen flow. These changes are associated with the Pd particles and are proposed to be due to a change in particle structure initiated by dissolution of Pd. During that process the catalytic activity remains largely intact. The study demonstrates that ATR-IR and UV–vis spectroscopy is a powerful combination for the study of catalytic solid–liquid interfaces in situ.

Acknowledgments

The Swiss National Science Foundation is acknowledged for funding of this project. We thank the mechanical workshop of the Institut de Physique, Université de Neuchâtel, for modification of the ATR-IR–UV–vis cell.

References

[1] B.M. Weckhuysen, J. Chem. Soc., Chem. Commun. (2002) 97.
[2] N.J. Harrick, Internal Reflection Spectroscopy, Interscience, New York, 1967.
[3] D. Ferri, T. Bürgi, A. Baiker, J. Phys. Chem. B 105 (2001) 3187.
[4] D. Ferri, T. Bürgi, J. Am. Chem. Soc. 123 (2001) 12,074.
[5] D. Ferri, T. Bürgi, A. Baiker, J. Chem. Soc., Chem. Commun. (2001) 1172.
[6] N. Bonalumi, T. Bürgi, A. Baiker, J. Am. Chem. Soc. 125 (2003) 13,342.
[7] T. Bürgi, A. Baiker, J. Phys. Chem. B 106 (2002) 10,649.
[8] T. Bürgi, R. Wirz, A. Baiker, J. Phys. Chem. B 107 (2003) 6774.
[9] T. Bürgi, M. Bieri, J. Phys. Chem. B 108 (2004) 13,364.
[10] C. Keresszegi, T. Bürgi, T. Mallat, A. Baiker, J. Catal. 211 (2002) 244.
[11] A. Gisler, T. Bürgi, A. Baiker, Phys. Chem. Chem. Phys. 5 (2003) 3539.
[12] M.K. Ko, H. Frei, J. Phys. Chem. B 108 (2004) 1805.
[13] A. Urakawa, R. Wirz, T. Bürgi, A. Baiker, J. Phys. Chem. B 107 (2003) 13,061.
[14] A. Bruckner, Catal. Rev.-Sci. Eng. 45 (2003) 97.
[15] R.L. Puurunen, B.G. Beheydt, B.M. Weckhuysen, J. Catal. 204 (2001) 253.
[16] M. Besson, P. Gallezot, Catal. Today 57 (2000) 127.
[17] T. Mallat, A. Baiker, Catal. Today 19 (1994) 247.
[18] P. Vinke, D. de Wit, A.T.J.W. de Goede, H. van Bekkum, in: P. Ruiz, B. Delmon (Eds.), New Developments in Selective Oxidation by Heterogeneous Catalysis, vol. 72, Elsevier, Amsterdam, 1992, p. 1.
[19] T. Mallat, A. Baiker, Chem. Rev. 104 (2004) 3037.
[20] J. Muzart, Tetrahedron 59 (2003) 5789.
[21] K. Nakamoto, Infrared and Raman Spectra of Inorganic and Coordination Compounds, fourth ed., Wiley, New York, 1986, 231 pp.
[22] S.E. Cabaniss, I.F. McVey, Spectrochim. Acta A 51 (1995) 2385.
[23] J.M.H. Dirkx, H.S. van der Baan, J. Catal. 67 (1981) 1.
[24] D. Ferri, T. Bürgi, A. Baiker, Helv. Chim. Acta 85 (2002) 3639.
[25] P. Sundararaman, E.C. Walker, C. Djerassi, Tetrahedron Lett. 19 (1978) 1627.
[26] J.L. Davis, M.A. Barteau, Surf. Sci. 197 (1988) 123.
[27] P. Vinke, H.E. van Dam, H. van Bekkum, in: G. Centi, F. Trifiro (Eds.), New Developments in Selective Oxidation, vol. 55, Elsevier, Amsterdam, 1990, p. 147.
[28] T. Mallat, A. Baiker, Catal. Today 24 (1995) 143.
[29] A. Mills, Chem. Soc. Rev. 18 (1989) 285.
[30] M. Hronec, Z. Cvengrosova, J. Tulejeva, J. Ilavsky, in: G. Centi, F. Trifiro (Eds.), New Developments in Selective Oxidation, vol. 55, Elsevier, Amsterdam, 1990, p. 169.
[31] P.J.M. Dijkgraaf, M.J.M. Rijk, J. Meuldijk, K. van der Wiele, J. Catal. 112 (1988) 329.
[32] P.J.M. Dijkgraaf, H.A.M. Duisters, B.F.M. Kuster, K. van der Wiele, J. Catal. 112 (1988) 337.
[33] H. Conrad, G. Ertl, J. Kuppers, E.E. Latta, Surf. Sci. 65 (1977) 245.
[34] A.B. Gaspar, L.C. Dieguez, Appl. Catal. A: General 201 (2000) 241.
[35] V. Arcoleo, M. Goffredi, A. Longo, V. Turco Liveri, Mater. Sci. Eng. C 6 (1998) 7.
[36] G. Mie, Ann. Phys. 25 (1908) 377.
[37] D.N. Furlong, A. Launikonis, W.H.F. Sasse, J. Chem. Soc., Faraday Trans. I 80 (1984) 571.
[38] W. Ostwald, Z. Phys. Chem. 22 (1897) 289.
[39] S.N. Sidorov, I.V. Volkov, V.A. Davanov, M.P. Tsyurupa, P.M. Valetsky, L.M. Bronstein, R. Karlinsey, J.W. Zwanziger, V.G. Matveeva, E.M. Sulman, N.V. Lakina, E.A. Wilder, R.J. Sponak, J. Am. Chem. Soc. 123 (2001) 10,502.
[40] Y. Schuurman, B.F.M. Kuster, K. van der Wiele, G.B. Marin, Appl. Catal. A 89 (1992) 47.